Chemistry & Biology, Vol. 11, 949–957, July, 2004, ©2004 Elsevier Ltd. All rights reserved. DOI 10.1016/j.chembiol.2004.04.020

Structural Transitions as Determinants of the Action of the Calcium-Dependent Antibiotic Daptomycin

David Jung,[1] Annett Rozek,[1] Mark Okon,[2] and Robert E.W. Hancock[1,*]
[1]Department of Microbiology and Immunology
[2]Department of Chemistry
University of British Columbia
232B-2259 Lower Mall
Vancouver, BC, V6T 1Z4
Canada

Summary

Daptomycin is a cyclic anionic lipopeptide antibiotic recently approved for the treatment of complicated skin infections (Cubicin). Its function is dependent on calcium (as Ca^{2+}). Circular dichroism spectroscopy indicated that daptomycin experienced two structural transitions: a transition upon interaction of daptomycin with Ca^{2+}, and a further transition upon interaction with Ca^{2+} and the bacterial acidic phospholipid, phosphatidyl glycerol. The Ca^{2+}-dependent insertion of daptomycin into model membranes promoted mild and more pronounced perturbations as assessed by the increase of lipid flip-flop and membrane leakage, respectively. The NMR structure of daptomycin indicated that Ca^{2+} induced a conformational change in daptomycin that increased its amphipathicity. These results are consistent with the hypothesis that the association of Ca^{2+} with daptomycin permits it to interact with bacterial membranes with effects that are similar to those of the cationic antimicrobial peptides.

Introduction

Daptomycin (brand name Cubicin in its injectable form) is a novel lipopeptide antibiotic that recently received New Drug Approval by the US FDA for the treatment of complicated skin infections caused by gram-positive organisms, including methicillin-resistant *Staphylococcus aureus* [1]. Another phase 3 trial is underway to examine its efficacy in the treatment of infective endocarditis and bacteraemia. In vitro studies have demonstrated that daptomycin has bactericidal activity against a wide variety of gram-positive bacteria, including vancomycin-resistant Enterococci, methicillin-resistant *Staphylococcus aureus*, coagulase-negative Staphylococci, glycopeptide intermediate-susceptible *Staphylococcus aureus*, and penicillin-resistant *Streptococcus pneumoniae* [2–6].

Antimicrobial peptides are ubiquitous in nature as components of host innate defense mechanisms against pathogenic microbes. However, the vast majority of these peptides are amphipathic and cationic, with charges of up to +9 conferred by excess arginine and lysine residues. In contrast, daptomycin is a negatively charged cyclic lipopeptide that is naturally produced as a fermentation end product from a strain of *Streptomyces roseosporus* [2]. The unique characteristic of daptomycin is that its antimicrobial activity is entirely dependent on calcium [4, 5, 7–9]. Two different mechanisms of action have been proposed for the bactericidal activity of daptomycin, involving either the inhibition of lipoteichoic acid (LTA) synthesis [10–12], which has been disputed [9, 13–15], or the dissipation of the membrane potential across the cytoplasmic membrane, leading to the disruption of several different cellular processes [14, 16]. Recently, Silverman et al. [13] proposed a multistep model for the mechanism of action of daptomycin that involves the depolarization of the cytoplasmic membrane. We were intrigued by this hypothesis as it has some similarities to a mechanism proposed by our laboratory for the cationic peptides [17].

In this study, we probed the effects of calcium on the structure of daptomycin and its interactions with membranes. Our results indicate that daptomycin undergoes two structural transitions, one of which we defined in detail through structural studies. On the basis of this structural and functional data, we propose a multistep interaction with membranes and a mechanism of action that expands on the previously proposed model by Silverman et al. [13].

Results and Discussion

The Role of Calcium in the Membrane Interaction of Daptomycin

Daptomycin is a cyclic lipopeptide that is composed of 13 amino acid residues, including three D-amino acids (D-asparagine-2, D-alanine-8, and D-serine-11), three uncommon amino acids [ornithine-6, (2S,3R)-3-methyl glutamic acid-12, and kynurenine-13], and an *n*-decanoyl fatty acid chain at the N-terminus [18] (Figure 1A). There are four acidic residues (three aspartic acid residues [3, 7, and 9] and one 3-methyl glutamic acid residue [12]) and one basic residue (ornithine [6]), resulting in a total molecular charge of −3 at neutral pH. The peptide is cyclic via formation of an ester bond between threonine-4 and kynurenine-13.

It has been clearly established that calcium plays an essential role in the antimicrobial activity of daptomycin (4, 5). We confirmed this here by demonstrating that, in the absence of calcium, daptomycin had a minimal inhibitory concentration (MIC) greater than 64 μg/ml, while in 0.34 mM, 2 mM, and 5 mM Ca^{2+} the MICs progressively decreased from 2 to 1 to 0.625 μg/ml, respectively, confirming the dependence of daptomycin activity on Ca^{2+}. Through fluorescence [7, 8] and fractionation [12] studies, it has been shown that daptomycin inserts and binds to membranes in a calcium-dependent manner. To see if this reflected structural transitions, we initially utilized circular dichroism (CD) spectroscopy (Figure 1B). Daptomycin in aqueous solution demonstrated an ellipticity maximum at a wavelength of 233 nm and a broad negative minimum at

*Correspondence: bob@cmdr.ubc.ca

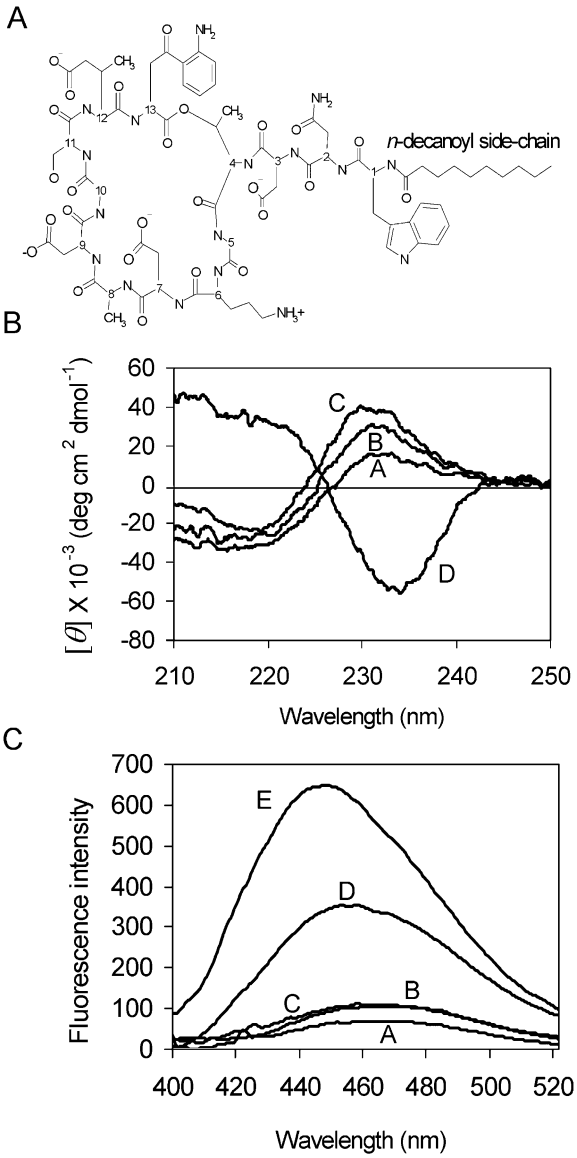

Figure 1. Chemical Formula, CD Spectra, and Fluorescence Emission Spectra of Daptomycin

(A) Chemical formula of daptomycin at neutral pH. The amino acid sequence of daptomycin is n-decanoyl-Trp-D-Asn-Asp-Thr-Gly-Orn-Asp-D-Ala-Asp-Gly-D-Ser-(2S, 3R) 3-MeGlu-Kyn.

(B) CD spectra of daptomycin in: A, aqueous solution; B, 5 mM $CaCl_2$ solution; C, PC/PG liposomes; and D, PC/PG liposomes and 5 mM $CaCl_2$ solution. The lipid to peptide molar ratio was 30:1, with a daptomycin concentration of 6 μM. Spectra are shown only between 210 and 250 nm because of extensive light scattering that occurred at lower wavelengths for every sample except A.

(C) Fluorescence emission spectra of daptomycin were recorded at an excitation wavelength of 375 nm in: A, aqueous solution in the absence of calcium and lipid; B, PC liposomes in the absence of 5 mM $CaCl_2$; C, mixed PC/PG liposomes in the absence of 5 mM $CaCl_2$; D, PC liposomes in the presence of 5 mM $CaCl_2$; and E, PC/PG liposomes in the presence of 5 mM $CaCl_2$. The lipid to peptide molar ratio was 30:1, with a daptomycin concentration of 10 μM.

210–220 nm. Preincubation of daptomycin with 5 mM $CaCl_2$ (hereafter referred to as Ca^{2+}) led to an increase in the positive ellipticity maximum and a slight shift to 231 nm. The addition to daptomycin of large unilamellar liposomes composed of a one-to-one mixture of the zwitterionic phospholipid phosphatidyl choline (PC) and the acidic phospholipid phosphatidyl glycerol (PG) in the absence of Ca^{2+} similarly led to a increase (as compared to aqueous daptomycin) in positive ellipticity combined with a slight blue shift. However, the addition of PC/PG liposomes in the presence of 5 mM Ca^{2+} caused the band at 233 nm to invert from a positive ellipticity to a negative ellipticity and the region between 210 nm and 220 nm to switch from a negative ellipiticity to a positive ellipticity. Large unilamellar PC liposomes in the presence of Ca^{2+} were not able to induce such an inversion of the CD spectrum (data not shown). The results indicated that daptomycin underwent a substantial conformational change when it associated with negatively charged membranes, which was dependent on the presence of Ca^{2+}.

Interaction of Daptomycin with Model Membranes

A variety of model membrane studies have been developed to assess the interactions of cationic peptides with membranes [19]. We used fluorescence spectroscopy to assess the insertion of daptomycin into membranes and study membrane perturbations such as lipid flip-flop and membrane leakage.

Daptomycin contains two aromatic residues (Trp-1 and Kyn-13) that are intrinsically fluorescent. Upon the insertion of these lipophilic residues into the phospholipid membrane, their environment becomes less polar, which causes a blue shift in the fluorescence emission wavelength combined with an increase in intensity [7, 8]. In aqueous solution, daptomycin in both the presence and absence of Ca^{2+} was weakly fluorescent, with an approximate maximum emission wavelength of 465 nm (Figure 1C). Addition of neutral PC liposomes in the presence of Ca^{2+} led to an 8 nm blue shift and a 5-fold increase in fluorescence intensity. Addition of acidic PC/PG (1:1) liposomes in the presence of Ca^{2+} led to a larger 16 nm blue shift and a 9-fold increase in fluorescence intensity. The addition of either PC or PC/PG liposomes to daptomycin in the absence of Ca^{2+} caused only minor changes in fluorescence. These results indicated that daptomycin inserted into bilayers of either acidic or neutral liposomes only in the presence of Ca^{2+} and that the insertion in mixed PC/PG liposomes was deeper than in PC liposomes.

The movement of lipid molecules between the bilayer leaflets (lipid flip-flop) provides one of the most sensitive measurements of peptide-lipid interactions [19, 20]. Lipid flip-flop was monitored with the fluorescent lipid probe C_6-NBD-PC. Daptomycin, in a Ca^{2+}-dependent manner, was able to induce substantial lipid flip-flop in both asymmetrically labeled acidic PC/PG (1:1) and neutral PC liposomes in a concentration-dependent manner (Figure 2A). Increasing the amount of Ca^{2+} from 2 to 5 mM increased the extent of lipid flip-flop. The extent of flip-flop began to plateau at around 0.5–2 μg/ml of daptomycin, equivalent to the MIC for many bacteria.

The ability of peptides to induce membrane leakage can be assessed by measuring the release of an encapsulated dye, calcein, from unilamellar vesicles [19–21].

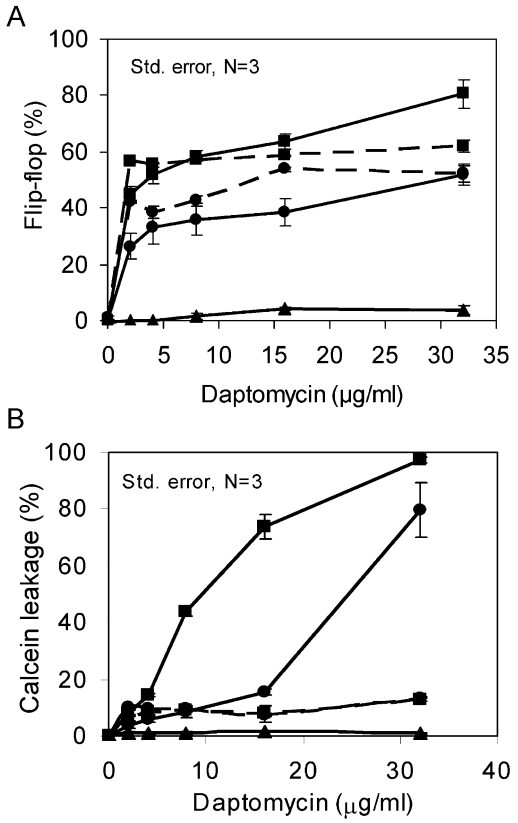

Figure 2. Lipid Flip-Flop and Calcein Leakage Caused by Daptomycin in Model Membranes

(A) Dose-dependent lipid flip-flop of the C_6-NBD-PC asymmetrically labeled PC/PG (solid lines) and PC (dashed lines) liposomes by daptomycin in the presence of 0 mM (▲), 2 mM (●) and 5 mM (■) $CaCl_2$.

(B) Dose-dependent calcein leakage from PC/PG (upper two solid lines) and PC (lower two dashed lines) liposomes caused by the addition of daptomycin with 0 mM (▲), 2 mM (●) and 5 mM (■) $CaCl_2$.

At the concentrations present inside liposomes, calcein self-quenches its own fluorescence; upon disintegration of the liposome membrane, calcein is released and its fluorescence dequenched. We assessed the ability of daptomycin to induce calcein leakage from both unilamellar PC/PG (1:1) and PC liposomes (Figure 2B). Daptomycin caused only 10% calcein leakage from neutral PC liposomes even at concentrations as high as 32 μg/ml. More significant calcein leakage was induced in acidic PC/PG liposomes, which increased with the Ca^{2+} concentration and occurred at peptide concentrations that were substantially higher than those causing lipid flip-flop. This dependence on acidic phospholipids was reminiscent of the structural transitions observed in CD studies where a major conformational change of daptomycin occurred only with PC/PG liposomes in the presence of Ca^{2+}. For the calcein release studies (Figure 2B), preincubation of daptomycin with Ca^{2+} was required to observe maximal effects. If the same concentrations of daptomycin and Ca^{2+} were separately added to the calcein-loaded PC/PG liposomes, less than 10% leakage of calcein was observed even at 16 μg/ml of daptomycin/5 mM Ca^{2+} (data not shown). No such requirement for preincubation was observed in lipid flip-flop experiments.

Structure of Ca^{2+}-free and Ca^{2+}-Conjugated Daptomycin

The addition of Ca^{2+} to the buffered daptomycin caused an increase in molecular ellipticity of the CD maximum at 233 nm (Figure 1B), and we confirmed, using fluorescence emission spectra, that membrane interaction, including neutral PC liposomes, was Ca^{2+} dependent (Figure 1C). These observations are consistent with the hypothesis that Ca^{2+} causes a structural change in daptomycin, which promotes lipid interaction. To examine this further, we analyzed the structures of daptomycin in the presence and absence of Ca^{2+} using two-dimensional homonuclear NMR spectroscopy. Resonance-specific chemical shift assignments of Ca^{2+}-free daptomycin (hereafter called apodaptomycin) and its Ca^{2+}-conjugated form were obtained using conventional NMR methods [22] (see Tables S1 and S2 in the Supplemental Data). Figure 3 shows the NOESY spectra at 25°C (τ_m = 150 ms) for apodaptomycin and Ca^{2+}-conjugated daptomycin. A comparison of these spectra shows clear differences for apodaptomycin versus Ca^{2+}-conjugated daptomycin. The resonances for the apopeptide were well resolved, whereas those for the Ca^{2+}-conjugated peptide were broadened. The increase in resonance linewidths may be due to intermediate chemical exchange between the Ca^{2+}-free and Ca^{2+}-bound peptide. Alternatively, the line broadening may indicate an increase in molecular weight due to peptide oligomerization [15]. Residues Trp-1 and Kyn-13 suffered the biggest increase in linewidth. The amide resonance of Trp-1 was not observed for Ca^{2+}-conjugated daptomycin, since it merged with the base line. The increase in resonance linewidths was accompanied by some chemical shift changes. The largest chemical shift change observed was 0.1 ppm for the Kyn-13 amide resonance. The similarity of chemical shifts suggests that there were no major conformational changes between the Ca^{2+}-bound and -unbound peptides. However, the NOESY spectra showed distinct differences in the pattern of NOE crosspeaks. For example, new NOE contacts were observed for Ca^{2+}-conjugated daptomycin between the *n*-decanoyl fatty acid chain and the side chains of Trp-1, D-Asn-2, and Kyn-13 (Figure 3B, boxed region). Together with the above-average increase in resonance linewidth for Trp-1 and Kyn-13, this data indicated that the interactions between these residues were enhanced in the presence of Ca^{2+}. To better describe the structural transition of daptomycin in the presence of Ca^{2+}, the structures of apodaptomycin and Ca^{2+}-conjugated daptomycin were determined. NOE-based distance restraints were collected from the NOESY spectra at 17°C (τ_m = 150 ms) (Figure S1) and 35°C (τ_m = 150 ms) (Figure S2), respectively. The adjustments in acquisition temperature were made to optimize the spectral resolution and the signal-to-noise ratio of NOE crosspeaks. An overview of the NOE restraints used to calculate the proposed three-dimensional structures of daptomycin in the absence and presence of Ca^{2+} is shown in Figure

A

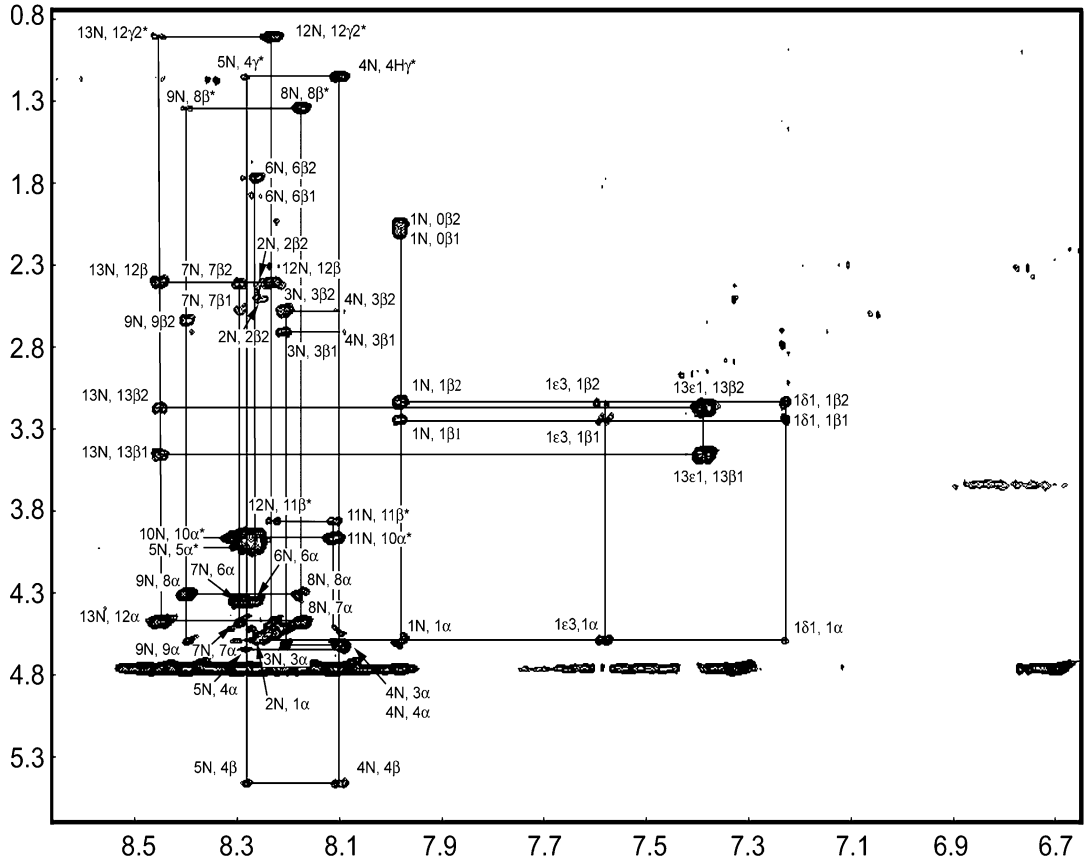
13N, 12γ2*
12N, 12γ2*
5N, 4γ*
4N, 4Hγ*
9N, 8β*
8N, 8β*
6N, 6β2
6N, 6β1
1N, 0β2
1N, 0β1
2N, 2β2
13N, 12β
7N, 7β2
12N, 12β
3N, 3β2
4N, 3β2
7N, 7β1
9N, 9β2
2N, 2β2
4N, 3β1
3N, 3β1
1N, 1β2
1ε3, 1β2
13ε1, 13β2
1δ1, 1β2
13N, 13β2
1δ1, 1β1
1N, 1β1
1ε3, 1β1
13N, 13β1
13ε1, 13β1
12N, 11β*
11N, 11β*
10N, 10α*
11N, 10α*
5N, 5α*
6N, 6α
9N, 8α
7N, 6α
8N, 8α
8N, 7α
13N, 12α
1N, 1α
1ε3,1α
1δ1, 1α
9N, 9α
7N, 7α
3N, 3α
5N, 4α
2N, 1α
4N, 3α
4N, 4α
5N, 4β
4N, 4β
0.8
1.3
1.8
2.3
2.8
3.3
3.8
4.3
4.8
5.3
8.5
8.3
8.1
7.9
7.7
7.5
7.3
7.1
6.9
6.7

B

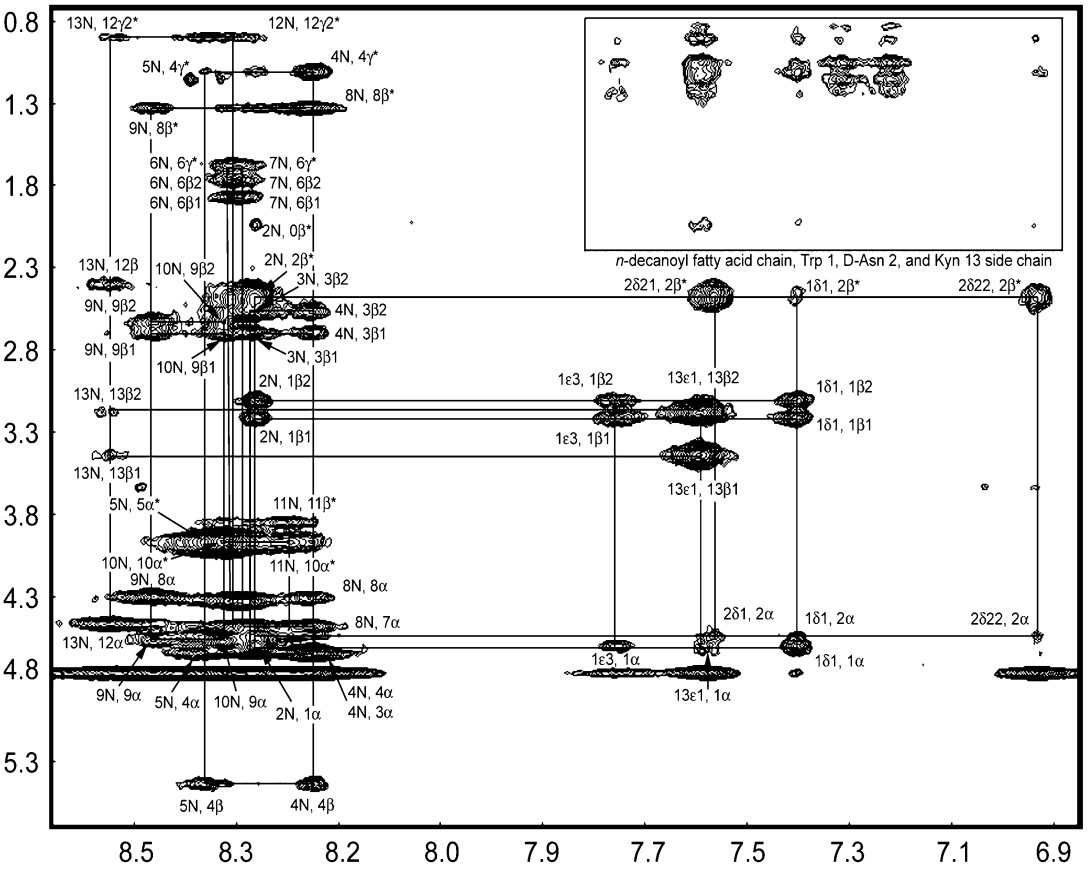
13N, 12γ2*
12N, 12γ2*
5N, 4γ*
4N, 4γ*
8N, 8β*
9N, 8β*
6N, 6γ*
7N, 6γ*
6N, 6β2
7N, 6β2
6N, 6β1
7N, 6β1
2N, 0β*
13N, 12β
10N, 9β2
2N, 2β*
3N, 3β2
9N, 9β2
4N, 3β2
4N, 3β1
9N, 9β1
10N, 9β1
3N, 3β1
2N, 1β2
13N, 13β2
2N, 1β1
13N, 13β1
5N, 5α*
11N, 11β*
10N, 10α*
11N, 10α*
9N, 8α
8N, 8α
8N, 7α
13N, 12α
9N, 9α
5N, 4α
10N, 9α
2N, 1α
4N, 4α
4N, 3α
5N, 4β
4N, 4β
n-decanoyl fatty acid chain, Trp 1, D-Asn 2, and Kyn 13 side chain
2δ21, 2β*
1δ1, 2β*
2δ22, 2β*
1ε3, 1β2
13ε1, 13β2
1δ1, 1β2
1δ1, 1β1
1ε3, 1β1
13ε1, 13β1
2δ1, 2α
1δ1, 2α
2δ22, 2α
1ε3, 1α
1δ1, 1α
13ε1, 1α
0.8
1.3
1.8
2.3
2.8
3.3
3.8
4.3
4.8
5.3
8.5
8.3
8.2
8.0
7.9
7.7
7.5
7.3
7.1
6.9

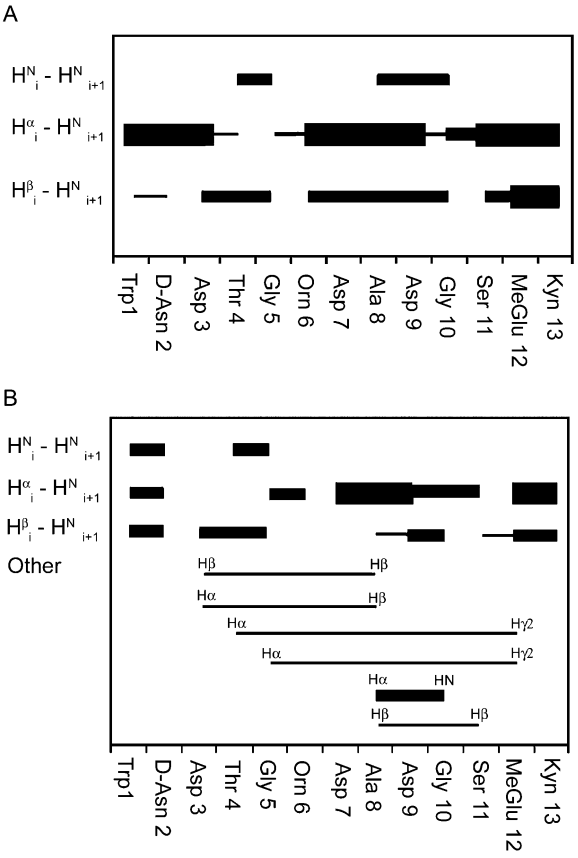

Figure 4. NOE-Derived Restraints

Summary of the NOE-derived distance restraints used to generate the structures of apodaptomycin (A) and Ca^{2+}-conjugated daptomycin (B). The thickness of the bars corresponds to the strength of the NOE restraints, which were grouped into strong, medium, and weak, with upper bounds up to 3.0 Å, 4.0 Å, and 5.0 Å, respectively.

4, and a statistical summary of the structure calculation is given in Table 1. For apodaptomycin, only sequential NOEs were observed, whereas the NOESY spectra of the Ca^{2+}-bound peptide showed a number of medium and long-range NOE connectivities. As a result, the structure of Ca^{2+}-conjugated daptomycin was much better defined. The backbone RMSD was reduced from 1.95 Å in apodaptomycin to 1.07 Å for Ca^{2+}-conjugated daptomycin (Table 1). Figures 5A and 5B show the superposition of the backbone of the structures calculated for apodaptomycin and Ca^{2+}-conjugated daptomycin, illustrating the higher degree of convergence for the Ca^{2+}-bound peptide. The backbone of apodaptomycin formed two bends at Asp-7 and Asp-9 and a highly variable region centered at Gly-5.

The binding of Ca^{2+} to daptomycin caused the ring structure to be drawn closer together by NOE restraints connecting Asp-3 with Ala-8, Thr-4 and Gly-5 with MeGlu-12 (three and four residues apart in the ring structure), and Ala-8 with Gly-10 and Ser-11. A type IV turn was formed between Thr-4 and Ala-8 (n + 1, $\phi = 72°$, $\psi = -157°$; n + 2, $\phi = -27°$, $\psi = -166°$). The side chain of Asp-3 was "tucked under" the ring structure due to the NOE restraints between the Asp-3 and the Ala-8 side chain (Figures 4, 5C, and 5D). The arrangement of the Asp-3 side chain suggests that this residue may be involved in the coordination of the Ca^{2+}-ion [23]. As for other Ca^{2+} binding proteins [24], the binding of Ca^{2+} to daptomycin resulted in a more constrained structure (i.e., the backbone average pairwise rmsd to the mean coordinates for the Ca^{2+}-conjugated structure was approximately half of the apostructure; Table 1). The high backbone variability in the apostructure around Gly-5 may reflect a function for this region as a flexible hinge, which would provide the conformational freedom required to permit for Asp-3 to move closer to the ring structure in order to participate in the coordination of Ca^{2+} in the Ca^{2+}-conjugated structure.

Calcium-induced changes have been linked to the exposure of hydrophobic residues that are crucial in the function of calcium-dependent proteins like annexinV [25, 26] and calmodulin [27]. Figures 5E and 5F illustrate the surface structures of apo- and Ca^{2+}-conjugated daptomycin. The total charge of the Ca^{2+}-conjugated peptide (−1) is lower than that of the apopeptide (−3) because of the binding of Ca^{2+}. In addition to the total charge reduction, an increase in amphipathicity was observed in the Ca^{2+}-conjugated daptomycin structure as compared to the apostructure due to the redistribution of charged side chains toward the top of the ring structure and the orientation of the Asp-3 side chain toward the center of the ring. The calcium-induced changes in the daptomycin structure led to an increase in the solvent-exposed hydrophobic surface from 943 Å^2 to 987 Å^2 and a decrease in the solvent-exposed hydrophilic surface from 1090 Å^2 to 945 Å^2, corresponding to a relative increase of the hydrophobic face of 5% (see Table S3). The clustering of the N-terminal lipid chain with Trp-1 and Kyn-13 was recognized from the NOESY spectra of Ca^{2+}-bound daptomycin but was not realized in the calculated structure because of the inability to assign the individual hydrocarbon chain resonances. The total charge reduction of daptomycin combined with the increase in amphipathicity and, to a lesser extent, the increase in hydrophobic surface upon binding of Ca^{2+} may promote peptide oligomerization, which may contribute to the resonance line broadening observed in the NMR spectra (Figure 3).

Membrane Depolarization Studies

Previous research into the mechanism of action of daptomycin indicated that treatment of susceptible

Figure 3. NOESY Spectra of Apodaptomycin and Ca^{2+}-Conjugated Daptomycin

NOESY spectra for apodaptomycin (A) and Ca^{2+}-conjugated daptomycin (B) were recorded at 25°C (pH 6.6 and 6.7, respectively) at a mixing time of 150 ms. NOE crosspeaks between the backbone amide protons, α-protons, and side-chain protons are labeled. The boxed region in (B) contains NOEs between the *n*-decanoyl fatty acid chain and the aromatic side chains of Trp-1 and Kyn-13 and the side chain amide protons of D-Asn-2, which were not specifically assigned. The residue number 0 refers to the *n*-decanoyl fatty acid chain on the N terminus.

Table 1. Statistical Analysis for the NMR-Derived Structures of Apodaptomycin and Ca^{2+}-Conjugated Daptomycin

	Apodaptomycin		Ca^{2+}-Conjugated Daptomycin	
No. of NOE restraints	82		86	
Interresidue	35		44	
Intraresidue	47		42	
No. of NOE restraint violations > 0.1 Å[a]	69 ± 3		54 ± 3	
Average highest NOE restraint violation (Å)[a]	0.26 ± 0.03		0.17 ± 0.02	
	Average Pairwise Rmsd to the Mean[a,b] (Å)			
	Backbone	Heavy Atom	Backbone	Heavy Atom
Residue no.				
1–13	1.95 ± 0.09	3.08 ± 0.13	1.07 ± 0.05	2.09 ± 0.07
4–13	1.15 ± 0.10	3.04 ± 0.13	0.78 ± 0.04	1.48 ± 0.04
3–8	1.22 ± 0.09	2.16 ± 0.12	0.58 ± 0.02	1.29 ± 0.07

Structures were calculated using the DGII program in Insight II v.97.2 (Accelrys, San Diego, CA).
[a] Expressed as mean ± standard deviation of 15 (apodaptomycin) and 17 (Ca^{2+}-conjugated daptomycin) accepted structures of 40 calculated.
[b] Calculated using MOLMOL 2K.2 [37].

S. aureus cells with 100 μg/ml daptomycin resulted in the dissipation of membrane potential [14], while daptomycin-resistant strains of *S. aureus* had an altered membrane potential [9]. More recently, a correlation between membrane depolarization and the bactericidal activity of daptomycin against growing *S. aureus* was observed

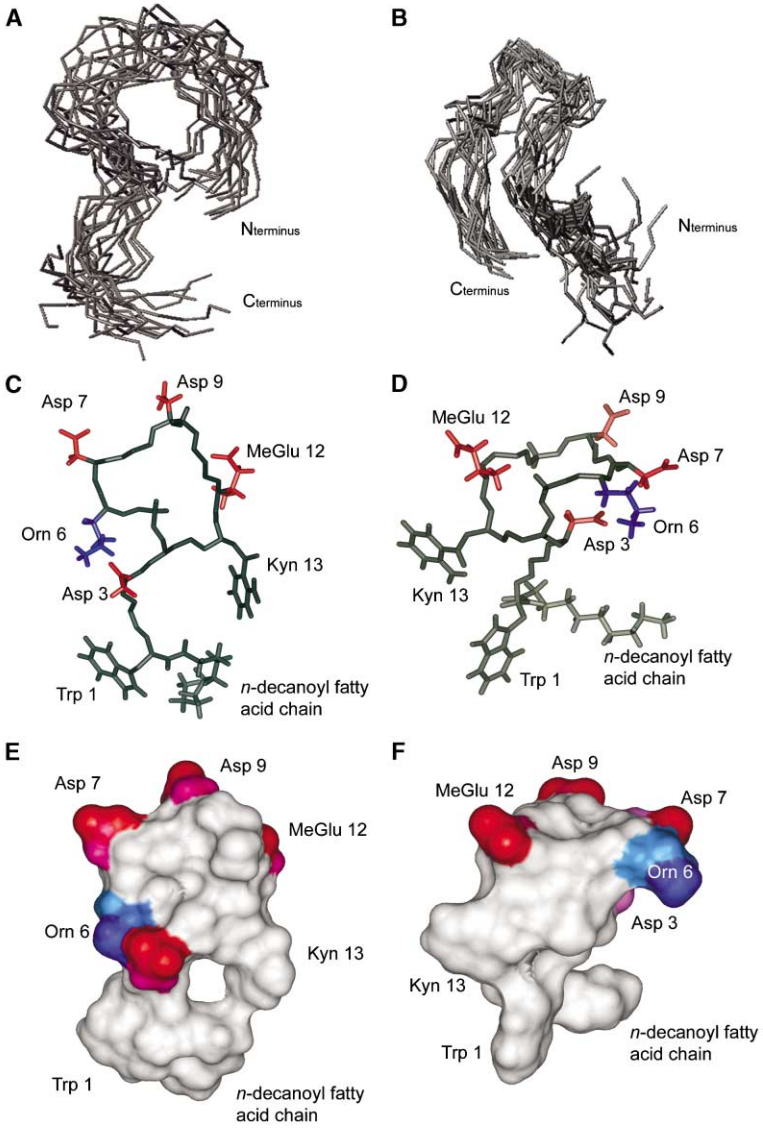

Figure 5. Structures of Apodaptomycin and Ca^{2+}-Conjugated Daptomycin

(A and B) Backbone representations of the ensembles of 15 accepted structures for apodaptomycin (A) and of 17 accepted structures for Ca^{2+}-conjugated daptomycin (B). The structures were superimposed using the backbone atoms between residues 1 and 13.
(C and D) Model of the apostructure (C) and Ca^{2+}-conjugated structure (D) closest to the average, with negatively charged side chains colored red and positively charged side chains colored blue.
(E and F) Surface representation of the apostructure (E) and Ca^{2+}-conjugated structure (F). The surface charge is color coded, with red representing negative charges and blue representing positive charges. Uncharged regions are shown in white.
Selected residues were labeled. (A) and (B) were prepared using MOLMOL 2K.2 [37], while (C), (D), (E), and (F) were prepared using Insight II v.97.2 (Accelrys Inc., San Diego, CA).

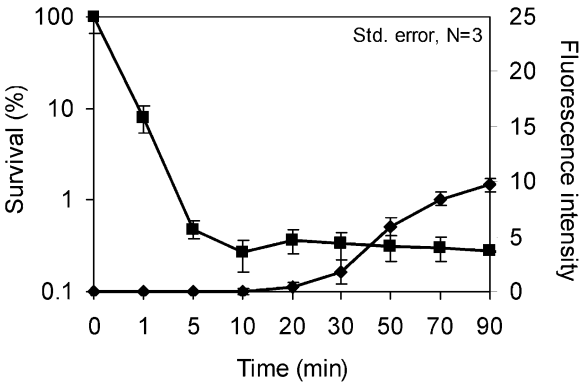

Figure 6. Relationship between Cytoplasmic Membrane Depolarization and Killing of *S. aureus* Caused by Daptomycin

The cytoplasmic membrane depolarization (◆) was measured at discrete times over a period of 90 min using the membrane potential-sensitive dye, $DiSC_35$. Bacterial survival (■) over the 90 min was estimated at discrete times by colony counts. Both experiments were done in parallel.

at 2-fold the minimal inhibitory concentration [13]. In this study, the viability of daptomycin-treated nongrowing *S. aureus* was assessed concurrently with membrane depolarization measured with the membrane potential-sensitive cyanine dye, 3,5-dipropylthiacarbocyanine ($DiSC_35$) [13]. We utilized in these studies 10-fold the MIC of daptomycin, since lower concentrations of daptomycin, closer to the MIC, showed no depolarization of nongrowing cells within the 90 min tested. When *S. aureus* was treated with 10 μg/ml of daptomycin/5 mM $CaCl_2$, 99% bacterial killing but only 36% membrane depolarization was observed within 90 min (Figure 6). The majority of the killing occurred within the first 10 min, whereas membrane depolarization was not evident until 20 min. This delay between the bactericidal affects of daptomycin and the start of membrane depolarization indicated that depolarization may be a consequence rather than the cause of bacterial death.

Significance

We demonstrated here that Ca^{2+} is required for two distinct conformational changes, each of which separately impacted how daptomycin interacted with membranes. Recently, Silverman et al. [13] proposed a multistep model for the mechanism of action of daptomycin. In their model, Ca^{2+} initially binds to daptomycin that is weakly bound to the cytoplasmic membrane and causes a conformational change that leads to the insertion and subsequent oligomerization of daptomycin within the membrane. On the basis of the studies reported here, we propose significant modifications to this model. The *S. aureus* cytoplasmic membrane contains both neutral and acidic phospholipids. Initially, Ca^{2+} binds to daptomycin in solution and causes a conformational change that increases amphipathicity and decreases its charge, thus allowing daptomycin to interact with either neutral or acidic membranes (as reflected by our fluorescence and lipid flip-flop measurements). Subsequently, Ca^{2+} may act as a bridge between daptomycin and acidic phospholipids, leading to a second conformational change that promotes deeper insertion of daptomycin into the membrane and large membrane perturbations, as indicated by our CD spectroscopy and calcein release studies. This two-step model would explain how this anionic peptide gains access to and interacts with bacterial cytoplasmic membranes. Silverman et al. [13] have argued that the bactericidal activity of daptomycin is due to cytoplasmic membrane depolarization caused by the leakage of intracellular ions, such as K^+. Although, in our hands, daptomycin was able to induce membrane leakage in liposomes, our observation that cytoplasmic membrane depolarization (in nongrowing cells) occurred subsequently to cell death indicates that it may not be the cause of cell death. Rather, we propose that the mechanism of action of daptomycin may involve multiple targets, as proposed previously for cationic peptides [17, 28–30]. Several other calcium-dependent lipopeptide antibiotics are known, including amphomycin, calcium-dependent antibiotic (CDA), and fruilimicin [31]. It is tempting to speculate that, since these antibiotics are thematically similar, they might share similar kinds of interactions with calcium and membranes.

Experimental Procedures

Liposome Preparation

Large unilamellar liposomes composed of 1-palmitoyl-2-oleoyl-*sn*-glycero-3-phosphocholine (PC) or an equimolar mixture of PC and 1-palmitoyl-2-oleoyl-*sn*-glycero-3-phospho-*rac*-1-glycerol (PG) (Avanti Polar Lipids Inc., Alabaster, AL) liposomes were prepared by resuspension of a dried lipid film in 20 mM HEPES buffer (pH 7.4), four freeze-thaw cycles, and extrusion through 0.1 μm filters as previously described [19].

Circular Dichroism Spectroscopy

CD spectra were recorded with 6 μM daptomycin in 20 mM HEPES buffer (pH 7.4) using a Jasco J-810 spectropolarimeter (Jasco Corp., Tokyo, Japan). The Ca^{2+}-conjugated daptomycin samples were preincubated with 5 mM $CaCl_2$. Large unilamellar liposomes were added to a final concentration of 180 μM lipid. Spectra were recorded at room temperature from 190 to 250 nm using a quartz cuvette with a 1 mm path length at a scan rate of 50 nm/min and a band width of 0.1 nm; spectra were the average of ten scans. Each spectrum was baseline corrected by subtracting a blank spectrum, and ellipticities were converted to mean residue molar ellipticities in units of deg × cm^2/dmol using Jasco software.

Fluorescence Spectroscopy

Fluorescence spectra were recorded with 10 μM daptomycin in 20 mM HEPES buffer (pH 7.4) using a Perkin-Elmer 650-10S fluorescence spectrometer (Perkin Elmer Inc., Norwalk, CT). Spectra were acquired at room temperature from 400 to 520 nm at an excitation wavelength of 365 nm with the slit width set to 5 nm. The Ca^{2+}-conjugated daptomycin samples were preincubated with 5 mM $CaCl_2$. Large unilamellar liposomes were added to a final concentration of 300 μM lipid. Each spectrum was baseline corrected by subtracting a blank spectrum.

Lipid Flip-Flop and Calcein Release

Lipid flip-flop experiments employing large unilamellar liposomes that were asymmetrically labeled with 0.5 mol% 1-palmitoyl-2-[6-((7-nitrobenz-2-oxa-1,3-diazol-4-yl)amino)-caproyl]-L-α-phosphatidyl choline (C_6-NBD-PC) (Avanti Polar Lipids Inc., Alabaster, AL) were performed exactly as described [19]. Calcein release experiments were done using large unilamellar liposomes with entrapped calcein exactly as described previously [19]. Daptomycin samples

were preincubated with 5 mM $CaCl_2$ for 1 hr prior to the experiment. Lipid flip-flop and calcein release are relative to Triton X-100.

NMR Spectroscopy and Structure Calculation

Daptomycin was provided by Cubist Pharmaceuticals. The apodaptomycin NMR sample contained 2 mM daptomycin, 100 mM KCl, 0.2 mM EDTA, 1 mM EGTA, and 7% D_2O (pH 6.6). The Ca^{2+}-conjugated daptomycin NMR sample contained 2 mM daptomycin, 100 mM KCl, 0.2 mM EDTA, 5 mM $CaCl_2$, and 7% D_2O (pH 6.7). NMR spectra were recorded on Varian Unity500 or Inova600 spectrometers operated by the UBC Laboratory for Molecular Biophysics. Homonuclear TOCSY (spin lock time = 60 ms) [32], NOESY (τ_m = 150 ms) [33], and DQF-COSY [34] spectra were initially collected at 25°C. Additional TOCSY and NOESY spectra were collected for apodaptomycin at 17°C (τ_m = 150 ms) and for Ca^{2+}-conjugated daptomycin at 30°C (τ_m = 150 ms) and 35°C (τ_m = 150–250 ms).

All NMR spectra were processed using NMRPipe [35] and analyzed using NMRVIEW v.5.0.4 [36]. NOE crosspeaks for apodaptomycin were integrated in the 17°C NOESY spectrum (τ_m = 150 ms). NOE crosspeaks for Ca^{2+}-conjugated daptomycin were integrated in the 35°C NOESY spectrum (τ_m = 150 ms) and further supplemented by additional NOE crosspeaks from the 25°C NOESY spectrum (τ_m = 150 ms) after both spectra were compared for any indications of conformational differences. Conversion of NOE volumes to distance restraints and pseudoatom corrections were calculated as described [29]. Structure calculations were performed using the DGII module of Insight II v.97.2 (Accelrys Inc., San Diego, CA). Calculated structures were accepted based on the lowest NOE distance restraint violations and best convergence. The structures were further analyzed using MOLMOL v.2K.1 [37].

Cytoplasmic-Membrane Depolarization and Bacterial Killing

The depolarization of the cytoplasmic membrane of *S. aureus* by daptomycin was determined with the membrane potential-sensitive dye 3,5-dipropylthiacarbocyanine ($DiSC_35$) (Molecular Probes, Eugene, OR) as previously described [17]. Briefly, *S. aureus* cells were grown to mid-log phase and then washed and resuspended in 5 mM HEPES/20 mM glucose buffer to a final OD_{600} of 0.05. The suspension was equilibrated in 0.4 μM $DiSC_35$ and 100 mM KCl until the fluorescence (excitation at 622 nm, emission at 670 nm) was completely quenched. Daptomycin (10 μg/ml) and 5 mM $CaCl_2$ were added, and the increase in fluorescence due to membrane depolarization and dye release was recorded. Bacterial viability was assessed in parallel by plating aliquots withdrawn from an identical cell suspension at the same time points to final dilutions of 10^{-3} and 10^{-4} and counting the bacterial colonies grown overnight.

Supplemental Data

Supplemental Data including two figures and three tables are available at http://www.chembiol.com/cgi/content/full/11/7/949/DC1.

Acknowledgments

We would like to acknowledge Jon-Paul Powers and Jared Silverman for useful discussions. Cubist Pharmaceuticals, Inc. provided financial assistance and daptomycin; additional financial contributions came from the Canadian Bacterial Diseases Network. R.E.W.H. held a Canada Research Chair, while A.R. was a CIHR Fellow.

Received: January 9, 2004
Revised: March 26, 2004
Accepted: April 26, 2004
Published: July 23, 2004

References

1. Raja, A., LaBonte, J., Lebbos, J., and Kirkpatrick, P. (2003). Fresh from the pipeline. Daptomycin. Nat. Rev. Drug Discov *2*, 943–944.
2. Tally, F.P., Zeckel, M., Wasilewski, M.M., Carini, C., Berman, C.L., Drusano, G.L., and Olseon, F.B.J. (1999). Daptomycin: a novel agent against gram-positive infections. Exp. Opin. Investig. Drugs *8*, 1222–1238.
3. Tally, F.P., and DeBruin, M.F. (2000). Development of daptomycin for gram-positive infections. J. Antimicrob. Chemother. *46*, 523–526.
4. Jones, R.N., and Barry, A.L. (1987). Antimicrobial activity and spectrum of LY146032, a lipopeptide antibiotic, including susceptibility testing recommendations. Antimicrob. Agents Chemother. *31*, 625–629.
5. Eliopoulos, G.M., Willey, S., Reiszner, E., Spitzer, P.G., Caputo, G., and Moellering, R.C., Jr. (1986). In vitro and in vivo activity of LY 146032, a new cyclic lipopeptide antibiotic. Antimicrob. Agents Chemother. *30*, 532–535.
6. Fass, R.J., and Helsel, V.L. (1986). In vitro activity of LY146032 against staphylococci, streptococci, and enterococci. Antimicrob. Agents Chemother. *30*, 781–784.
7. Lakey, J.H., and Ptak, M. (1988). Fluorescence indicates a calcium-dependent interaction between the lipopeptide antibiotic LY146032 and phospholipid membranes. Biochemistry *27*, 4639–4645.
8. Lakey, J.H., Maget-Dana, H.R., and Ptak, M. (1989). The lipopeptide antibiotic A21978C has a specific interaction with DMPC only in the presence of calcium ions. Biochim. Biophys. Acta *985*, 60–66.
9. Silverman, J.A., Oliver, N., Andrew, T., and Li, T. (2001). Resistance studies with daptomycin. Antimicrob. Agents Chemother. *45*, 1799–1802.
10. Boaretti, M., Canepari, P., Lleo, M.M., and Satta, G. (1993). The activity of daptomycin on Enterococcus faecium protoplasts: indirect evidence supporting a novel mode of action on lipoteichoic acid synthesis. J. Antimicrob. Chemother. *31*, 227–235.
11. Boaretti, M., and Canepari, P. (1995). Identification of daptomycin-binding proteins in the membrane of Enterococcus hirae. Antimicrob. Agents Chemother. *39*, 2068–2072.
12. Canepari, P., Boaretti, M., del Mar Lleo, M., and Satta, G. (1990). Lipoteichoic acid as a new target for activity of antibiotics: mode of action of daptomycin (LY146032). Antimicrob. Agents Chemother. *34*, 1220–1226.
13. Silverman, J.A., Perlmutter, N.G., and Shapiro, H.M. (2003). Correlation of daptomycin bactericidal activity and membrane depolarization in Staphylococcus aureus. Antimicrob. Agents Chemother. *47*, 2538–2544.
14. Alborn, W.E., Allen, N.E., and Preston, D.A. (1991). Daptomycin disrupts membrane potential in growing Staphylococcus aureus. Antimicrob. Agents Chemother. *35*, 2282–2287.
15. Laganas, V., Alder, J., and Silverman, J.A. (2003). In vitro bactericidal activities of daptomycin against Staphylococcus aureus and Enterococcus faecalis are not mediated by inhibition of lipoteichoic acid biosynthesis. Antimicrob. Agents Chemother. *47*, 2682–2684.
16. Allen, N.E., Alborn, W.E., Jr., and Hobbs, J.N., Jr. (1991). Inhibition of membrane potential-dependent amino acid transport by daptomycin. Antimicrob. Agents Chemother. *35*, 2639–2642.
17. Friedrich, C.L., Moyles, D., Beveridge, T.J., and Hancock, R.E.W. (2000). Antimicrobial action of structurally diverse cationic peptides on gram-positive bacteria. Antimicrob. Agents Chemother. *44*, 2086–2092.
18. Debono, M., Barnhart, M., Carrell, C.B., Hoffmann, J.A., Occolowitz, J. L., Abbott, B.J., Fukuda, D.S., Hamill, R.L., Biemann, K., and Herlihy, W.C. (1987). A21978C, a complex of new acidic peptide antibiotics: isolation, chemistry, and mass spectral structure elucidation. J. Antibiot. *40*, 761–767.
19. Zhang, L., Rozek, A., and Hancock, R.E.W. (2001). Interaction of cationic antimicrobial peptides with model membranes. J. Biol. Chem. *276*, 35714–35722.
20. Matsuzaki, K., Murase, O., Fugii, N., and Miyajima, K. (1996). An antimicrobial peptide, Magainin *2*, induced rapid flip-flop of phospholipids coupled with pore formation and peptide translocation. Biochemistry *35*, 11361–11368.
21. Kobayashi, S., Takeshima, K., Park, C.B., Kim, S.C., and Matsuzaki, K. (2000). Interactions of the novel antimicrobial peptide buforin 2 with lipid bilayers: proline as a translocation promoting factor. Biochemistry *39*, 8648–8654.

22. Wüthrich, K. (1986). NMR of proteins and nucleic acids (New York: John Wiley & Sons, Inc.).
23. Yang, W., Lee, H.W., Hellinga, H., and Yang, J.J. (2002). Structural analysis, identification, and design of calcium-binding sites in proteins. Proteins *47*, 344–356.
24. Qin, Z., and Squier, T.C. (2001). Calcium-dependent stabilization of the central sequence between Met(76) and Ser(81) in vertebrate calmodulin. Biophys. J. *81*, 2908–2918.
25. Minks, C., Huber, R., Moroder, L., and Budisa, N. (1999). Atomic mutations at the single tryptophan residue of human recombinant annexin V: effects on structure, stability, and activity. Biochemistry *38*, 10649–10659.
26. Neumann, J.M., Sanson, A., and Lewit-Bentley, A. (1994). Calcium-induced changes in annexin V behaviour in solution as seen by proton NMR spectroscopy. Eur. J. Biochem. *225*, 819–825.
27. Ikura, M. (1996). Calcium binding and conformational response in EF-hand proteins. Trends Biochem. Sci. *21*, 14–17.
28. Xiong, Y.Q., Yeamen, M.R., and Bayer, A.S. (1999). In vitro antibacterial activities of platelet microbicidal protein and neutrophil and defensin against Staphylococcus aureus are influenced by antibiotics differing in mechanism of action. Antimicrob. Agents Chemother. *43*, 1111–1137.
29. Rozek, A., Friedrich, C.L., and Hancock, R.E. (2000). Structure of the bovine antimicrobial peptide indolicidin bound to dodecylphosphocholine and sodium dodecyl sulfate micelles. Biochemistry *39*, 15765–15774.
30. Hancock, R.E.W., and Rozek, A. (2002). Role of membranes in the activities of antimicrobial cationic peptides. FEMS Microbiol. Lett. *206*, 143–149.
31. Hojati, Z., Milne, C., Harvey, B., Gordon, L., Borg, M., Flett, F., Wilkinson, B., Sidebottom, P.J., Rudd, B.A., Hayes, M.A., et al. (2002). Structure, biosynthetic origin, and engineered biosynthesis of calcium-dependent antibiotics from Streptomyces coelicolor. Chem. Biol. *9*, 1175–1187.
32. Braunschweiler, L., and Ernst, R.R. (1983). Coherence transfer by isotropic mixing: application to proton correlation spectroscopy. J. Magn. Reson. *53*, 521–528.
33. Jeener, J., Meier, B.H., Bachmann, P., and Ernst, R.R. (1979). Investigation of exchange processes by two-dimensional NMR spectroscopy. J. Chem. Phys. *71*, 4546–4553.
34. Rance, M., Sorensen, O., Bodenhausen, G., Wagner, G., Ernst, R.R., and Wüthrich, K. (1983). Improved spectral resolution in cosy 1H NMR spectra of proteins via double quantum filtering. Biochem. Biophys. Res. Commun. *117*, 479–485.
35. Delaglio, F., Grzesiek, S., Vuister, G.W., Zhu, G., Pfeifer, J., and Bax, A. (1995). NMRPipe: A multidimensional spectral processing system based on UNIX pipes. J. Biomol. NMR *6*, 277–293.
36. Johnson, B., and Blevins, R.A. (1994). NMRView: a computer program for the visualization and analysis for NMR data. J. Biomol. NMR *4*, 603–614.
37. Koradi, R., Billeter, M., and Wüthrich, K. (1996). MOLMOL: a program for display and analysis of macromolecular structures. J. Mol. Graph. *14*, 51–55.

Accession Numbers

The NMR structures for apo and Ca^{2+}-conjugated daptomycin were submitted to the Protein Data Bank (accession numbers 1T5M and 1T5N, respectively). The chemical shifts for apo and Ca^{2+}-conjugated daptomycin were deposited in the BioMagResBank (BMRB) (accession numbers RCSB022341 and RCSB022342, respectively).